EGTRIB Journal
JOURNAL OF
THE EGYPTIAN SOCIETY OF TRIBOLOGY
VOLUME 12, NO. 2, April 2015, pp. 15 - 29 **ISSN 2090 - 5882**

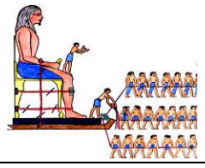

A NOVEL APPROACH FOR THE EFFECT OF THE HOUSING HEIGHT OF ANTI-FRICTION BEARINGS ON THE GENERATED VIBRATION USING DYNAMIC MODEL

Nabhan A.[1], Nouby M.[2], Sami A.M.[1] and Mousa M.O.[1]

[1]Prod. Eng. & Design Dept., Faculty of Eng., Minia University, 61111 Minia, Egypt
[2]Mech. Eng. Dept., Faculty of Eng., South Valley University, 83521 Qena, Egypt

ABSTRACT
The three-dimensional model of the housing and outer race is modeled in commercial package ABAQUS/CEA. An experimental acceleration results are given to make a comparison with the simulated acceleration signal obtained from the dynamic model. The influence of housing structure with different height 120, 100, 80, 60 and 40 mm is investigated, where the vibration response has been evaluated using the root mean square parameter RMS. It was found that, the housing with height of 40 mm displayed the lowest fluctuation in the output response. Also, bearing stability increased with the decrease of the bearing height, where the bearings with height 40 and 60 mm showed the best results.

KEYWORDS
Anti-friction bearings, Vibration analysis, RMS_A, RMS_D or RMS_D, dynamic model.

INTRODUCTION
Vibration analysis is among the most common method used in the monitoring applications since a defect produces successive impulses at every contact of defect and the rolling element, and the housing structure is forced to vibrate at its natural modes. The vibration pattern of a damaged bearing includes the low-frequency components related to the impacts and the high-frequency components. The structural information of the bearing structure or the machine is stored.

The effect of local defects on the nodal excitation functions is modeled. Simulated vibration signals are obtained, [1]. The signal analysis is applied to the simulated signals to obtain an indicator value for the defect. RMS values are obtained in the time domain and the high frequency resonance technique is used in the frequency domain. The indicator values are obtained for various rotational speeds, for different loading and housing structure. The indicator value from different signal processing methods which is most sensitive to the defect is found for different cases. Estimation of the running speed and the bearing key frequencies are required for failure detection and diagnosis. Experimental data were used to verify the validity of the algorithms. Data were collected through an accelerometer measuring the vibration from the drive-end ball bearing of an induction motor. Both inner and outer race defects were artificially introduced to the

bearing using electrical discharge machining, [2]. A linear vibration model was also developed for generating simulated vibration data. The simulated data were also used to validate the performance of the algorithms.

Dynamic loading model is proposed to model the localized rolling element bearing defects. Statistical properties of the vibration signals for healthy and defected structures are compared, [3]. The envelope high frequency resonance technique method is employed in the frequency domain analysis. The effect of the rotational speed on the diagnostics of rolling element bearing defects is investigated. An optimum sensor location on the structure is sought. Effect of the structure geometry on the monitoring techniques is studied. Time domain analysis, frequency domain analysis and spike energy analysis have been employed to identify different defects in bearings, [4]. Spike energy factor helps to identify the severity of the defect in antifriction bearings. The distinct and different behavior of vibration signals from bearings with inner race defect, outer race defect and roller defect helps in identifying the defects in roller bearings. The results have demonstrated that each one of these techniques is useful to detect problems in antifriction bearings.

The machine is a single stage centrifugal compressor with a rolling element thrust bearing on the motor free end and a sleeve bearing on the motor drive end. The expert system severity score is an excellent way to consistently trend the bearing health because it always applies the same logic and looks at a number of features in the data. The increase of the severity towards the extreme level and a bearing replacement is ordered. The defect was detected using off the shelf portable vibration analysis hardware and software, [5]. The partial correlation integral algorithm is used to analyze machine vibration data obtained throughout a life test of a rolling element bearing. The dimensional exponent computed from the partial correlation integral algorithm tends to increase as time progresses and the useful remaining life of the bearing is decreasing, [6]. The dimensional exponents of a healthy bearing and a bearing close to failure are statistically different. As a result, the condition of the bearing can be characterized from the results of the surrogate data test. Furthermore, the dimensional exponent can be used to predict the failure of rolling element bearings in rotating machinery from real-time vibration data.

A dynamic simulation method is proposed to study ball bearing with local defect based on the coupling of the piecewise function and the contact mechanism at the edge of the local defect, [7]. The ball bearing is simulated as a two-degree of freedom system. The impulse force is determined by the ratio of the ball size to the defect size and the contact deformation at the edge of the local defect is included. The proposed method can provide a more close to real impulse for the contact between the ball and the race with different defect sizes compared to the assumed rectangular or half-sine impulse function. The localized bearing defects in spindles were modeled visually. The vibration responses generated due to the outer ring defect were simulated. The finite element model of the spindle is capable of predicting the acceleration time responses due to the excitation, [8]. The noise decreases the amplitudes at the bearing characteristic frequencies in the envelop spectrum.

The detection of local defects existing on races of deep groove ball bearing was investigated using envelope analysis and Duffing oscillator. Experiments have been carried out using a test rig for capturing the vibration signals of test bearing. The

external vibration has been imparted to the housing of the test bearing through electromechanical shaker, [9]. The Duffing oscillator has acquired the weak defective bearing signal. The close phase plane trajectories of Duffing oscillator have confirmed the presence of the defects on the races of the test bearing. The scalar parameters, peak-to-peak value, RMS, Crest factor and kurtosis, show damage at the ball bearing but they do not give information about the location of defect. Therefore, spectrum analyses are conducted at specified test durations in order to predict defect locations, [10]. Vibration signatures produced are recorded and statistical measures are calculated during the test. Vibration spectra are obtained and examined to determine where the defect is on the running surfaces.

The vibration signals obtained from an accelerometer were measured and analyzed for comparative purposes. The time-domain statistical parameters and frequency-domain modified Peak Ratio were calculated and compared. The study revealed that ultrasound technique is demonstrably superior to vibration acceleration measurements for detecting incipient defects in low speed bearings, [11]. The RMS of ultrasound signals provided the best parameter at almost all speeds. However, at very low speeds, the kurtosis and crest factors performed best. In the frequency domain, a modified Peak Ratio was proposed and was proven to a better indicator than the original Peak Ratio. A simple time series method for bearing fault feature extraction using singular spectrum analysis of the vibration signal is proposed, [12]. The algorithms were evaluated using two experimental data sets one from a motor bearing subjected to different fault severity levels at various loads, with and without noise. The effect of sample size, fault size and load on the fault feature is studied. The experimental results demonstrate that the proposed bearing fault diagnosis method is simple, noise tolerant and efficient.

A finite element contact mechanics bearing model is established based on a contact algorithm suited to high-precision elastic, [13]. The computational model includes all the important bearing details besides basic geometry, such as, internal clearance, roller and race crowning, race width and thickness, and dimensions of the raceway shoulders. The computed stiffness matrix captures the coupling between radial, axial, and tilting deflections of rolling element bearings. The proposed stiffness determination method is validated the experiments and compared to existing analytical models. A method is presented for calculating and analyzing the quasi-static load distribution and varying stiffness of a radially loaded double row bearing with a raceway defect of varying depth, length, and surface roughness, [14]. The resonance frequency in the first vibration mode of mechanical system was studied, [15]. Under the assumption of a stepwise function for the envelope signal, the modulated signal could be decomposed into a sinusoidal function basis at the first vibration mode resonance frequency. According to the experimental study, the envelope detection method for the first vibration mode resonance frequency could be effectively applied in the signal processing for the bearing defect diagnosis.

A mathematical model for the ball bearing vibrations due to defect on the bearing race has been developed, [16]. It is found that, the amplitude level of vibrations for the case of outer race defect is more than that for the inner race defect and the ball defect. The defect present on the inner race moves in and out of the load zone during each revolution of the shaft. In this instance, the strong fault signatures produced while the defect is in the load zone are averaged with the weaker signatures acquired while the defect is outside the load zone. The theoretical model was aimed to study the effect of

defect size, load and speed on the bearing vibration and predict the spectral components.

Finite element model can be effectively used to differentiate between vibration signatures for defects of different sizes in the bearing, [17]. Assumptions have been made for the variation of forces exerted by the rolling element on the outer ring in the vicinity of the defect. Experiment result has been taken for the analysis of the signal that has been obtained through the use of FFT analyzer. The vibration signal response of the defected bearing is analyzed and compared with the normal bearing. The vibration signal pattern obtained from the simulation was found to have similar characteristics with experimental data.

A dynamic loading model simulates the distribution load in the outer race due to transfer load from the ball. Time domain analysis is performed to evaluate the output result of vibration analysis from the finite element software. RMS and peak to peak value is used as the time signal descriptors and can be used as a parameter for condition monitoring purposes. The vibration response of healthy and defected bearing is compared. The simulated vibration pattern has similar characteristics with results from experimental results, [18]. The effect of shaft rotational speed and radial load is investigated. The finite element model of a bearing and housing structure has been developed. Then the model is analyzed to obtain the vibration signal in the frequency domain, [19]. An analytical model is proposed to study the nonlinear dynamic behavior of rolling element bearing systems including surface defects, [20]. Various surface defects due to local imperfections on raceways and rolling elements are introduced to the proposed model. Mathematical expressions were derived for inner race, outer race and rolling element local defects. The validity of the proposed model verified by comparison of frequency components of the system response with those obtained from experiments.

The vibrations generated by deep groove ball bearings having multiple defects on races were studied, [21]. The vibrations are analyzed in both time and frequency domains. The equations for time delay between two or more successive impulses have been derived and validated with simulated and experimental results. The relationships between amplitudes of frequencies for impulse train, delayed impulse train and combination of two impulse trains have been established. Frequency spectra for single and two defects on either race of deep groove ball bearings are compared. Wavelet transform provides a variable resolution time-frequency distribution from which periodic structural ringing due to repetitive force impulses, generated upon the passing of each rolling element over the defect, were detected, [22]. A basic wavelet considered optimal for bearing localized defect detection is constructed. Finally, the scheme is described and its effectiveness is evaluated using actual vibration signals measured from bearings with defects at different locations and operating under different conditions.

The discrete wavelet transform can be used as an effective tool for detecting single and multiple faults in the ball bearings, [23]. Furthermore, discrete wavelet transform has been proposed for measuring outer race defect width of taper roller bearing. Experiments were carried out on a customized test setup, [24]. Vibration signals from ball bearings having single and multiple point defects on inner race, outer race, ball fault and combination of these faults have been considered for analysis, [25]. Wavelet transform provides a variable resolution time–frequency distribution from which periodic structural ringing due to repetitive force impulses, generated upon the passing

of each rolling element over the defect, are detected. The decomposed signal evidently splits the peak corresponding to the ball entry into and exit from the fault, enabling in an estimation of the defect size present in the bearing, [26]. Experiments conducted for different sizes of the defect present on the outer race of deep groove ball bearing affirm the efficacy of the applied technique for different vibration signals. The output of the proposed technique finds close correlation with the actual defect size measured from optical microscope

The aim of this study is to create a deep groove ball bearing model. Simulated vibration signals are obtained. The influence of housing structure with different height 120, 100, 80, 60 and 40 mm is investigated at zero clearance, ε = 0.5, by using the root mean square parameter RMS.

LOAD DISTRIBUTION

The loads carried by anti-friction bearings are transmitted through the rolling elements from one race to the other, [27]. The relationship between load and deflection is:

$$Q = K\delta^n \quad (1)$$

Where:

n : It is a constant which equal to 1.5 for ball bearings 1.11 for roller bearings.
Q : The normal load.
δ :is deformation.
K : Load/deflection factor.

For a rigidly supported bearing subjected to a radial load, the radial deflection at any angular position of the rolling element is given by:

$$\varepsilon = \frac{1}{2}\left(1 - \frac{P_d}{2\,\delta_r}\right) \quad (2)$$

Where,

δ_r : Radial shift of race, at $\psi = 0^0$,
ψ : The angular position, degree
P_d :The diametralclearance,
ε: The load distribution factor.

For ball bearingwith zero redial clearance and subjected to concentrated load, the load distribution can be determined from the following relation:

$$Q_\psi = Q_{max}\left[1 - \frac{1}{2\,\varepsilon}(1 - \cos\psi)\right]^n \quad (3)$$

$$Q_{max} = \frac{4.37\,F_r}{Z\cos\alpha} \quad (4)$$

Where,

F_r : The radial load
Z :The number of balls.

FINITE ELEMENT MODEL

The bearing type used in this study is a single row deep groove ball bearing 6004 (SKF). The bearing geometry is shown in Fig. 1. Its dimensions are:

- **Outer diameter, D_o = 42 mm**
- **Bore diameter,D_i = 20 mm**
- **Pitch diameter, d_m = 31 mm**
- **Raceway width, B = 12 mm**
- **Ball diameter, D = 6.35 mm**
- **Contact angle, α = 0°**
- **Raceway diameter of outer race, d_o = 34.8 mm**

- **Raceway diameter of inner race, d_i = 27.2 mm**

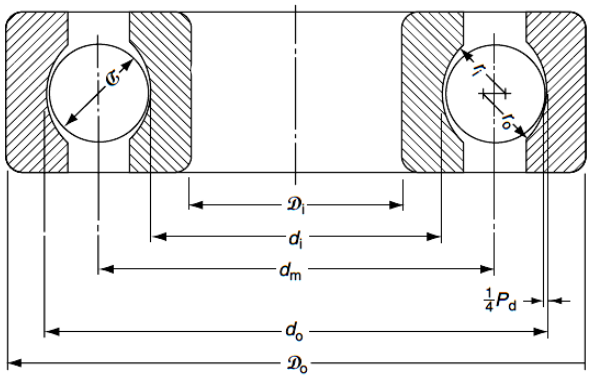

Fig. 1 Geometry of deep groove ball bearing Nr. 6004, [27].

To monitor the condition of the antifriction ball bearing, the finite element method is adopted to observe the dynamic response of the structure. The model is built as a three-dimensional model for the outer race and the housing. The step module provides the dynamic-explicit procedure to capture changes in the loading and boundary conditions of the model. It is assumed that, the contact between the outer surface of the outer race and its mating surface on the casing structure is ideal, which means that, no relative motion permitted on the contact surface. The three-dimensional model of the housing and outer race are simulated in commercial package ABAQUS/CEA. It assumed also that, the bearing material is isotropic and linear-elastic fracture mechanics with the following material characteristics has been considered:

- **Modulus of elasticity "E" = 203GPa,**
- **Poisson's ratio "ν" = 0.29**
- **Density "ρ" = 7850 Kg/m^3.**

The material of the bearing housing is assumed to be isotropic and linear-elastic fracture mechanics with the following properties has been used:

- **Modulus of elasticity "E" = 195GPa,**
- **Poisson's ratio "ν" = 0.26**
- **Density "ρ" = 7300 Kg/m^3.**

Figure 2 shows the dynamic model with two set measure points, on which the frequency will be determined. The inner surface of the housing hole and the outer surface of the bearing outer race are defined as a tie constrains. The housing part is fixed in three mutual perpendicular displacement directions (U1, U2, U3); mainly x-, y- and z-direction; as well as it is non-rotational about these axis(UR1, UR2, UR3). The load acting on each node along the inner circumference of the loading zone of the outer raceway have to be developed. The mesh of explicit elements with reduced integration and eight nodes (C3D8R) are used. Both housing and race define with the element type but using different global size.

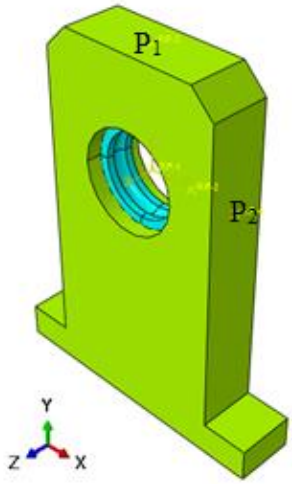

Fig. 2 Three-dimensional model of the housing with outer race of bearing.

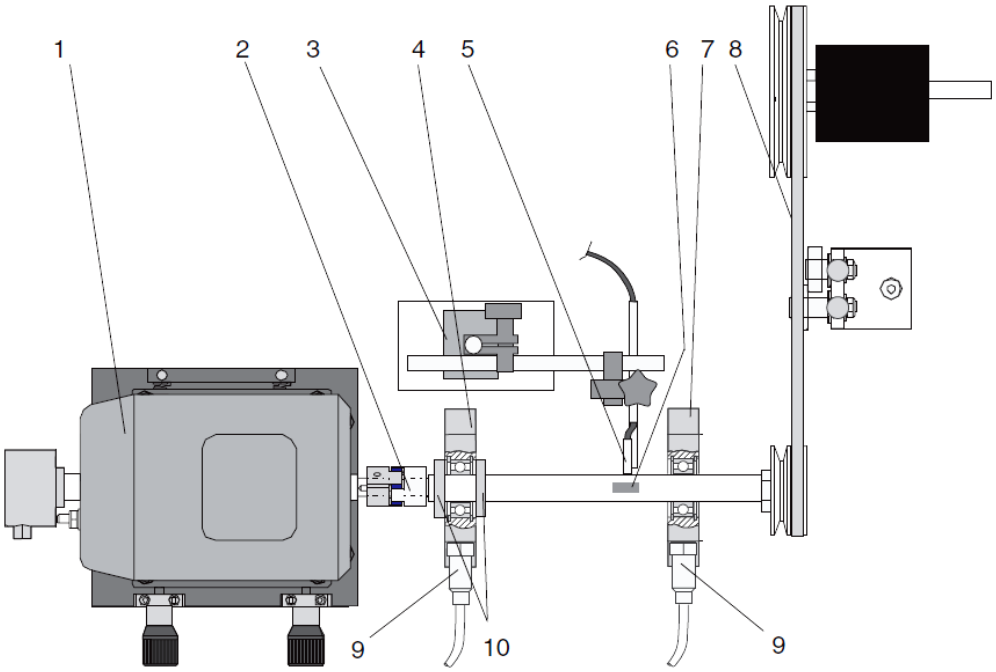

1. Drive unit
2. Elastic claw coupling.
3. Magnetic clamp with steel plate.
4. Bearing block;
5. Reference sensor.
6. Short shaft with reflective mark;
7. Bearing block.
8. Belt drive.
9. Acceleration sensor.
10. Setting ring.

Fig. 3.1 Schematic representation of the test rig.

TIME DOMAIN TECHNIQUES

A simple detection and a normal diagnostic approach is to analyze the measured vibration signal in the time domain. A more sophisticated approach can be used such as trending time domain of statistical parameters. Here, number of statistical parameters can be defined such as root mean square "RMS" which based upon the beta distribution. The "RMS" parameter can be defined with the following relation:

$$RMS = \sqrt{\frac{1}{N}\sum_{i=1}^{N}[X(t) - \bar{X}]} \qquad (5)$$

Where,

- $\bar{X}$ **: The mean value of the discrete time signal X (t).**
- **N : Number of data points.**

EXPERIMENTAL SET-UP

An experimental setup is employed in this work to collect the vibration signals to study the vibration signatures, that generated by incipient bearing defects. The test rig and the equipment used in collecting the data is shown in Fig. 3. The system is driven by a variable motor with speed up to 6000 rpm. An optical encoder is used for the speed measurement. An elastic claw coupling is utilized to damp out the high-frequency vibration generated by the motor. Two ball bearings are fitted into the solid housings. Accelerometers (IMI Sensors- 603C01) are mounted on the housing of the tested bearing to measure the vibration signals along two directions. A variable load is applied by a belt drive where the signal collection is carried out by a data acquisition card.

VALIDATION BETWEEN THE EXPERIMENTAL AND SIMULATION RESULTS

The boundary conditions of the simulation process have been chosen to satisfy an acceptable homogeneity between the experimental set up and the simulated model. Fig.4 shows an experimental acceleration signalfor a healthy bearing and a bearing with a defected outer race, while the corresponding signal; that obtained from the simulation process; is shown in Fig.5.It is observed from Figures 4a and 5a that the dynamic response of the healthy bearing is approximately similar for the experimental and theoretical cases.

Furthermore, it is noticed for the case of bearing with defected outer race that, the experimental results of Fig. 4b confirm that of the defected bearing; i.e. Fig. 5b. These results indicated that the proposed method of simulation can be used to produce vibration data for condition monitoring applications. However, the difference between the experimental and simulation signals may be due to the interval time used in dynamic model which has the value of 0.0001sec.

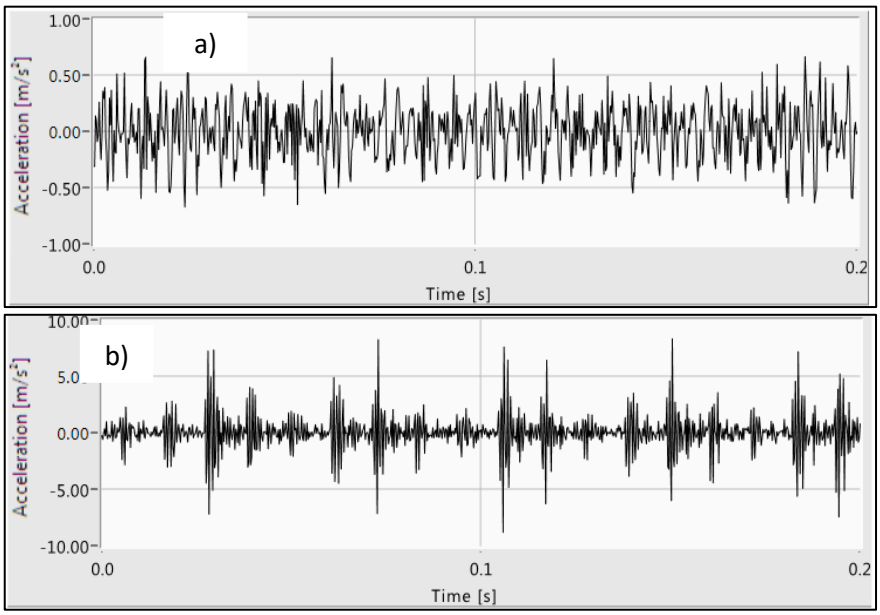

(a) Healthy bearing.
(b) Bearing with defected outer race.

Fig. 4 Experimental Acceleration signals for bearings.

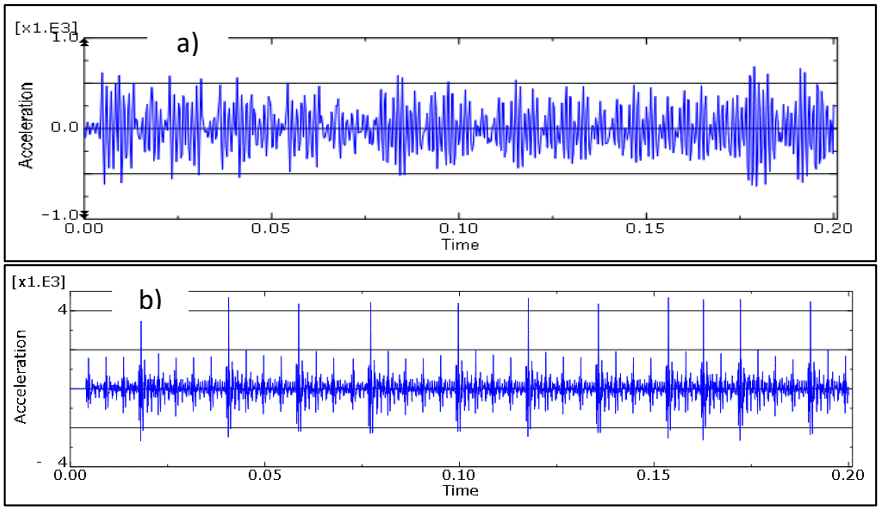

(a) Healthy bearing.
(b) Bearing with defected outer race.

Fig. 5 Acceleration response at horizontal point, 1500 rpm.

The experimental results showed the ratio between the root mean square "RMS" of the acceleration of the defected bearing to that of the healthy one "R_{RMS}". Figure 6 illustrates the RMS-ratio of the acceleration "R_{RMS}" for bearing with outer race defect versus the shaft speed. The RMS-ratio in the vertical direction displays higher values than that of the horizontal direction. Also, the value of the RMS-ratio decreases with the increase of the shaft speed. It is important to notice that, the higher values of the RMS-ratio on the vertical direction is connected to the position of the defect of the outer race, which means that the RMS-ratio increases at the position of the outer race defect.

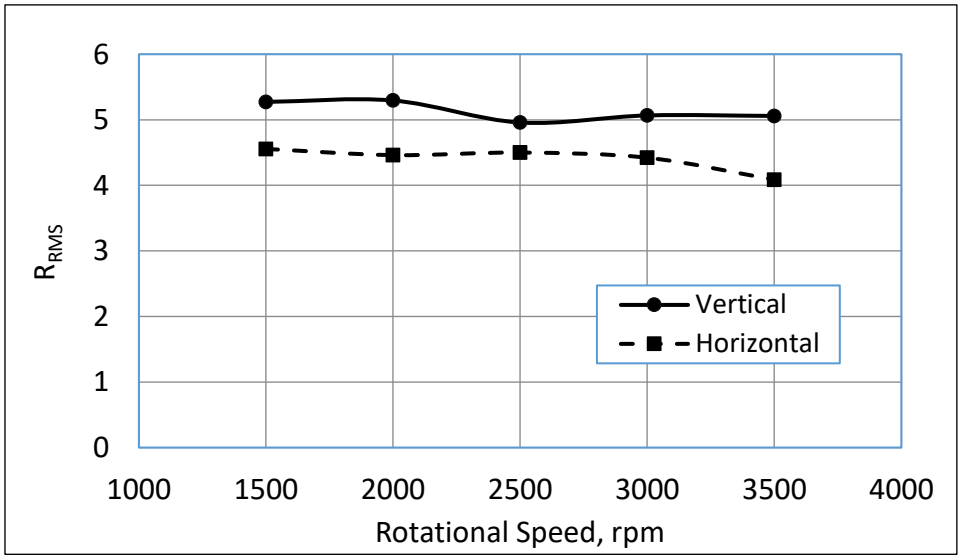

Fig. 6 Experimental variation of the acceleration RMS-ratio versus shaft speed for bearing with outer race defect.

The analytical results described the alteration of the bearing acceleration, velocity and displacement. Fig. 7 illustrates the variation of the RMS-ratio of the acceleration versus the shaft speed. The value of the RMS-ratio at point "P_1", i.e. in the vertical direction; is small in comparison to the horizontal one. Also, the RMS-ratio decreases with the

increase of the shaft speed. Therefore, it is easier to detect the bearing defect at low speeds than that by high speeds which can be due to the reduction of the pulse interval. The comparison between the simulation and experiment results shows a good agreement between the results. However, the variation between the experimental and the simulation values may be due to the inequality of the defect size in both cases.

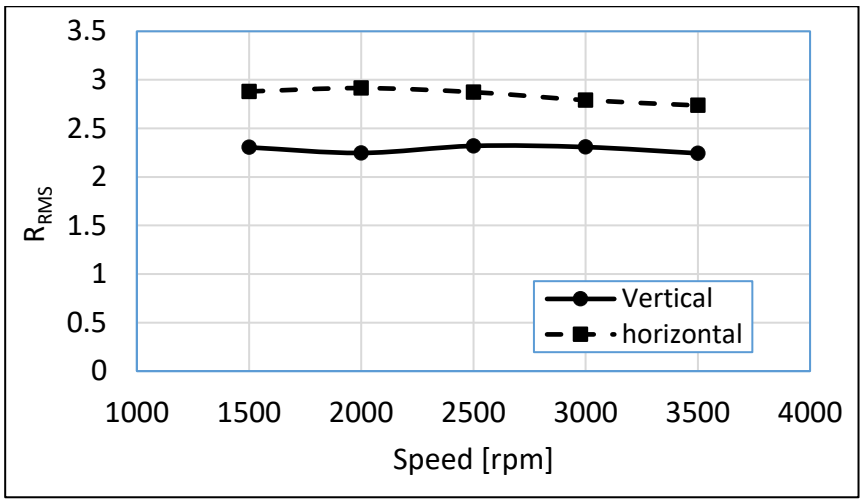

Fig. 7 Analytical variation of the acceleration RMS-ratio versus shaft speed for bearing model with outer race defect.

EFFECT OF BEARING HOUSING HEIGHT

The relation between the root mean square of the acceleration "RMS_A" for point "P_1" and the shaft speed is illustrated in Fig.8 for different bearing housing heights. It is clear that, the housing with heights of 120 and 100 mm shows high fluctuation for the acceleration signal. However, the housing with height of 40 mm displays the most balanced configuration. The same observation is valid for the horizontal direction; i.e. at point "P_2" as shown in Fig.9. Also, the vertical direction; "i.e. P_1"; gives results, which are greater than that of the horizontal direction; i.e.at point P_2.

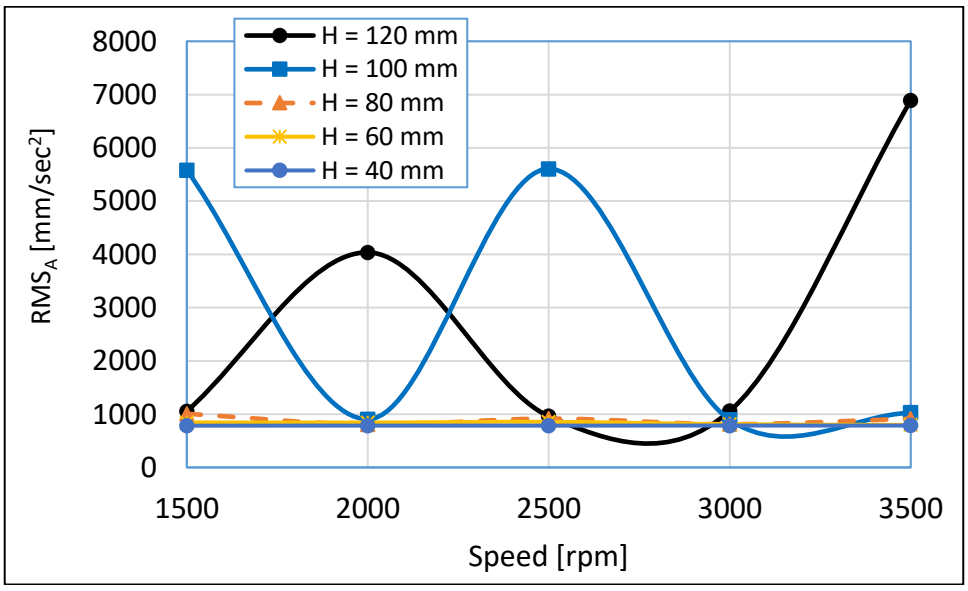

Fig. 8 RMS_A response of point "P_1" versus shaft speed at different heights.

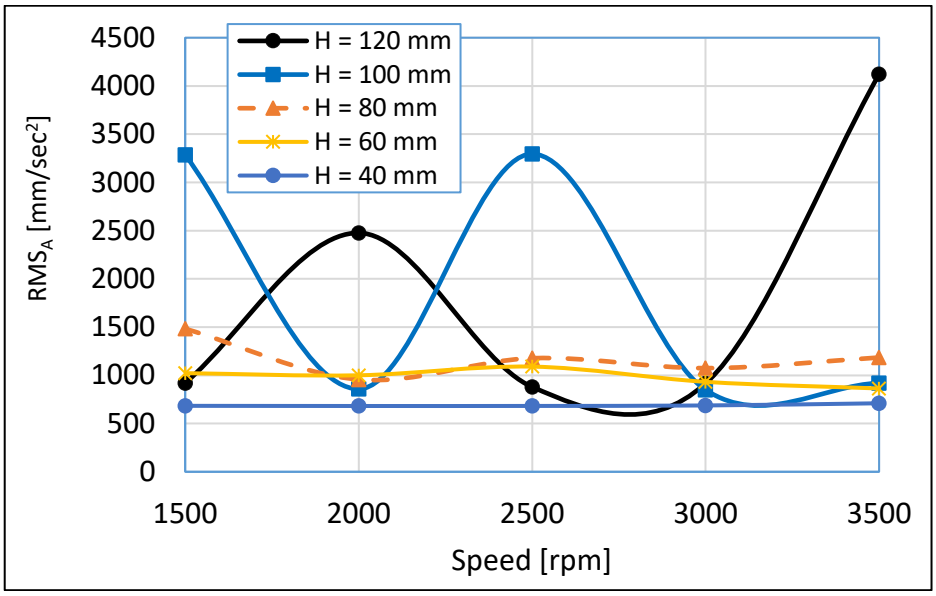

Fig.9 RMS$_A$ response of point "P$_2$" versus shaft speed at different housing heights.

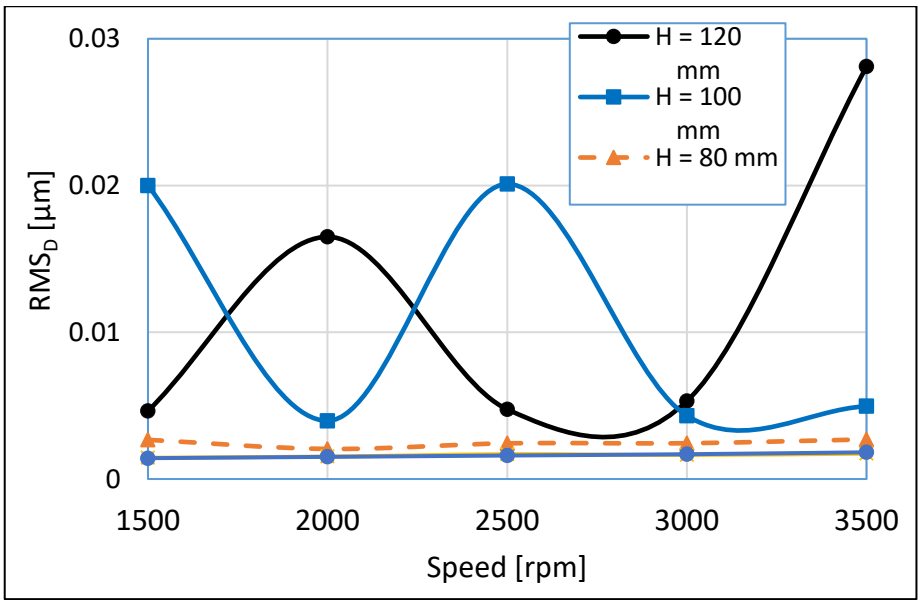

Fig. 10 RMS$_D$ response of point "P$_1$" versus shaft speed at different housing heights.

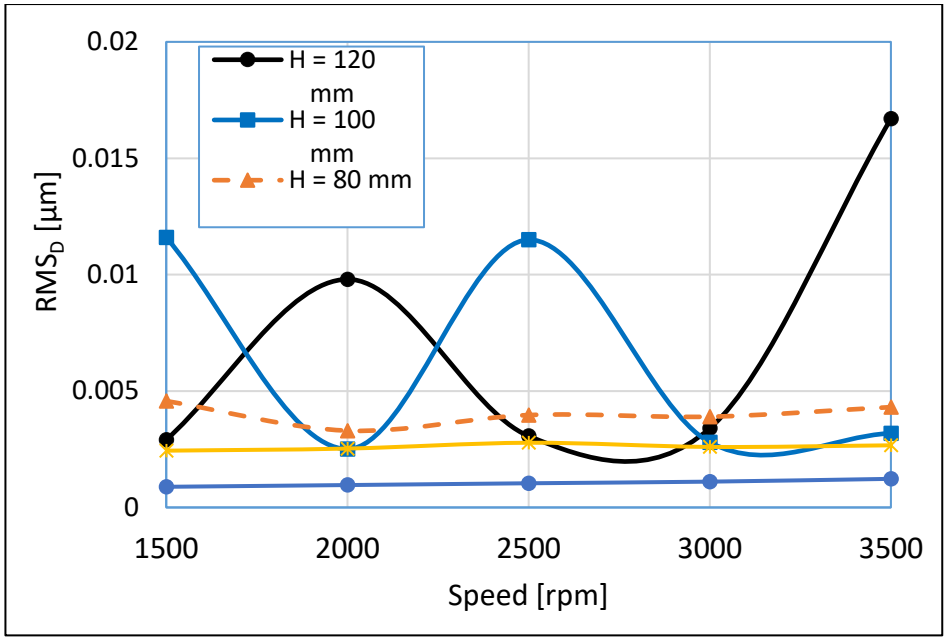

Fig. 11 RMS$_D$ response of point "P$_2$" versus shaft speed at different housing heights.

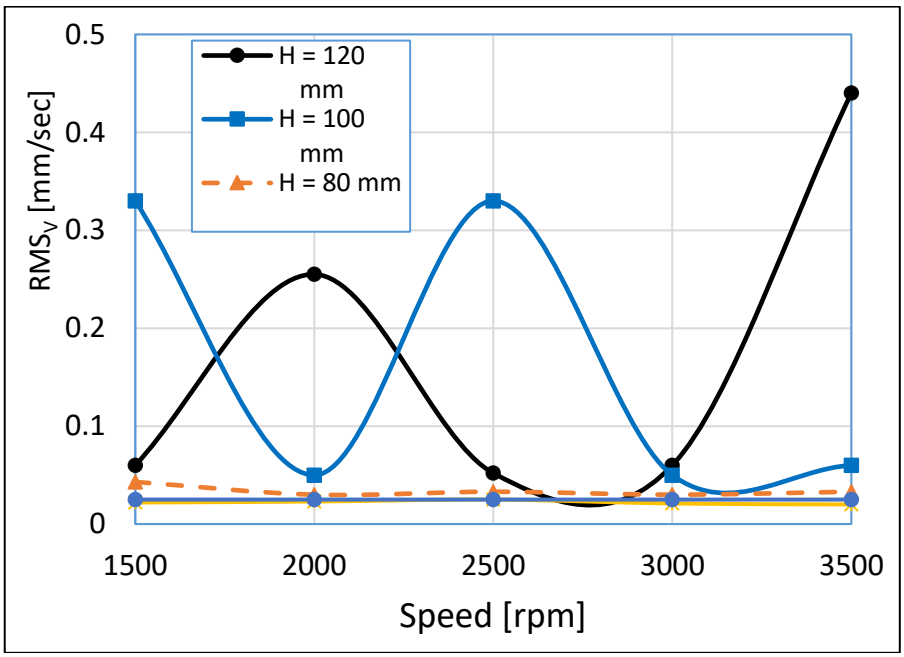

Fig. 12 RMS$_V$ response of point "P$_1$"versus shaft speed of different housing heights.

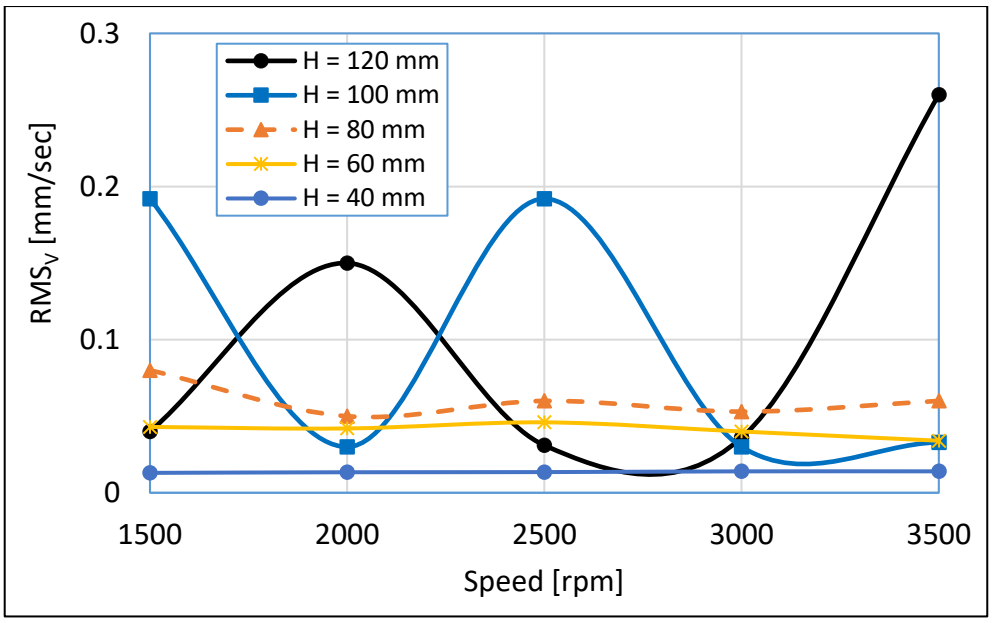

Fig. 13 RMS$_V$ response at point "P$_2$" versus shaft speed at different housing heights.

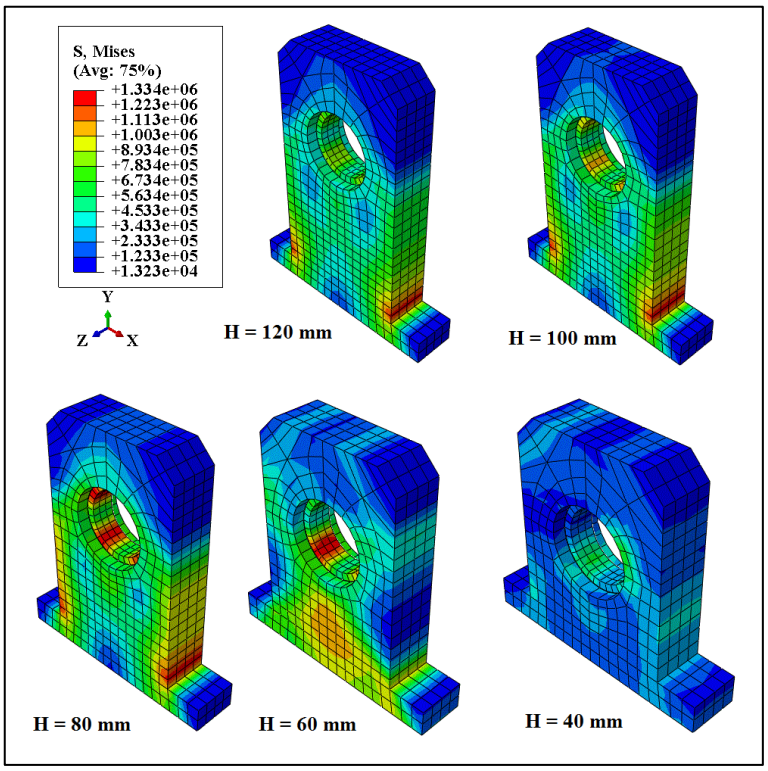

Fig. 14 Distribution of the stresses for bearings with different housing heights.

Figures 10 & 11 show the dependence of the root mean square of the displacement signal "RMS$_D$" for different housing heights versus the shaft speed for the vertical and horizontal points "P$_1$, P$_2$" respectively. Also, the dependence of the root mean square of

the velocity signal "RMS_V" for different housing heights versus the shaft speed are shown in Figures 12 &13 for the vertical and horizontal points "P_1, P_2" respectively. It is important to notice that, the variation of the RMS_D and RMS_V shows high fluctuation with the shaft speed for the housing with heights of 120 and 100 mm. The housing with the smallest high of 40 mm displays the lowest fluctuation in the output response. In general, short bearings display the most suitable conditions of obtaining running with high balance, Fig.20 shows an example for the distribution of the stresses where the bearing with height 40 mm shows the best results.

CONCLUSIONS

Based on the results from the dynamic model and according to the great agreement between the experimental results and that obtained from ABAQUS/CAE package, the following conclusions can be drawn:

1. **Bearing vibration can be characterized accurately with one of the root mean square parameters which describe the acceleration, displacement or velocity response, i.e., RMS_A, RMS_D or RMS_D.**
2. **The housing with heights of 40 mm displayed the lowest fluctuation in the output response.**
3. **Bearing stability increased with the decrease of the bearing height, where the bearings with the height 40 and 60 mm showed the best results.**

REFERENCES

1. **Kiral Z. "Simulation and Analysis of Vibration Signals Generated by Rolling Element Bearings with Defects", Ph. D. Thesis. The University of Izmir, Turkey, (2002).**
2. **Hasan O., Kenneth A. L., "Estimation of the running speed and bearing defect frequencies of an induction motor from vibration data", Mechanical Systems and Signal Processing, VOL. 18, pp. 515–533, (2004).**
3. **Kiral Z., Karagulle H., "Simulation and analysis of vibration signals generated by rolling element bearing with defects", Tribology International, VOL. 36, pp. 667–678, (2003).**
4. **Amarnath M., Shrinidhi R., Ramachandra A., Kandagal S. B., "Prediction of Defects in Antifriction Bearings using Vibration Signal Analysis", IE (I) Journal-MC, (2004).**
5. **Michael S. Johnson Jr., P.E., "Vibration Tests for Bearing Wear", ASHRAE Journal, (2000).**
6. **Janjarasjitta S., Ocak H., Loparo K. A., "Bearing condition diagnosis and prognosis using applied nonlinear dynamical analysis of machine vibration signal", Journal of Sound and Vibration, 317, pp. 112–126, (2008).**
7. **Jing L., Yimin S., Teik C. L., "Vibration analyses of ball bearings with a localized defect applying piecewise response function", Mechanism and Machine Theory, 56, pp. 156–169, (2012).**
8. **Hongrui C., Linkai N. , Zhengjia H., "Method for Vibration Response Simulation and Sensor Placement Optimization of a Machine Tool Spindle System with a Bearing Defect", Sensors, 12, pp. 8732-8754, (2012).**
9. **Patel V. N., Tandon N., Pandey R. K., "Defect detection in deep groove ball bearing in presence of external vibration using envelope analysis and Duffing oscillator", Measurement, 45, pp. 960–970, (2012).**
10. **Tuncay K., Nizami A., "Experimental diagnostics of ball bearings using statistical and spectral methods", Tribology International, 42, pp. 836–843, (2009).**

11. **Yong-Han K., Andy C. C. T., Joseph M., Bo-Suk Y., "Condition Monitoring of Low Speed Bearings: A Comparative Study of the Ultrasound Technique versus Vibration Measurements", WCEAM, (2006).**
12. **Bubathi M., Sanjith M. A., Krishnakumar B., Satya S. A., "Roller element bearing fault diagnosis using singular spectrum analysis", Mechanical Systems and Signal Processing, 35, pp. 150–166, (2013).**
13. **Yi G., Robert G. P., "Stiffness matrix calculation of rolling element bearings using a finite element/contact mechanics model", Mechanism and Machine Theory, 51, pp. 32–45, (2013).**
14. **Dick P., Carl H., Nader S., Alireza M. A., Sarabjeet S., "Analysis of bearing stiffness variations, contact forces and vibrations in radially loaded double row rolling element bearings with raceway defects", Mechanical Systems and Signal Processing, 50-51, pp. 139–160, (2015).**
15. **Yuh-Tay S., "An envelope analysis based on the resonance modes of the mechanical system for the bearing defect diagnosis", Measurement, 43, pp. 912–934, 2010.**
16. **Patil M. S., Jose M., Rajendrakumar P. K., Sandeep Desai, "A theoretical mode to predict the effect of localized defect on vibrations associated with ball bearing", International Journal of Mechanical Sciences, 52, pp. 1193–1201, (2011).**
17. **Patel U. A., Shukla R., "Vibrational Analysis of Self Align Ball Bearing Having a Local defect through FEA and its Validation through Experiment", International Journal of Modern Engineering Research, 2, pp. 1073-1080, (2012).**
18. **Purwo K., Zahari T., "Vibration Analysis of Defected Ball Bearing using Finite Element Model Simulation", The 9th Asia Pasific Industrial Engineering & Management Systems Conference, (2008).**
19. **Zahari T., Nguyen T. D., "Rolling Element Bearing Fault Detection with a Single Point Defect on the Outer Raceway Using FEA", The 11th Asia Pasific Industrial Engineering & Management Systems Conference, (2010).**
20. **Ahmad R., Saeed A., AnoushiravanFarshidianfar, Hamid Moeenfard, "Nonlinear dynamic modeling of surface defect sin rolling element bearing systems", Journal of Sound and Vibration, 319, pp. 1150–1174, (2009).**
21. **Patela V. N., Tandonb N., Pandey R. K., "Vibrations Generated by Rolling Element Bearings having Multiple Local Defects on Races", Procedia Technology, Vol. 14, pp. 312–319, (2014).**
22. **James L. C., Jun M., "Wavelet decomposition of vibrations for detection of bearing-localized defects", NDT & E International, 30, pp. 143-149, (1997).**
23. **Prabhakar S., Mohanty A. R., Sekhar A. S, "Application of discrete wavelet transform for detection of ball bearing race faults", Tribology International, 35, pp. 793–800, (2002).**
24. **Rajesh K., Manpreet S., "Outer race defect width measurement in taper roller bearing using discrete wavelet transform of vibration signal", Measurement, 46, pp. 537–545, (2013).**
25. **Purushotham V., Narayanan S., Suryanarayana A. N. P., "Multi-fault diagnosis of rolling bearing elements using wavelet analysis and hidden Markov model based fault recognition", NDT &E International, 38, pp. 654–664, (2005).**
26. **Khanam S., Tandon N., Dutt J. K., "Fault Size Estimation in the Outer Race of Ball Bearing Using Discrete Wavelet Transform of the Vibration Signal", Procedia Technology, Vol. 14, p.p. 12–19, (2014).**
27. **Tedric A. H., Michael N. K., "Essential Concepts of Bearing Technology", 5th edition, Taylor & Francis Group, (2006).**